

RESEARCH PAPER



Fusobacterium nucleatum promotes colorectal cancer metastasis by modulating KRT7-AS/KRT7

Shujie Chen^{a,b,*}, Tingting Su^{a,b,*}, Ying Zhang^{a,b,*}, Allen Lee^c, Jiamin He^{a,b}, Qiwei Ge^{b,d}, Lan Wang^{a,b}, Jianmin Si^{a,b}, Wei Zhuo^{b,e}, and Liangjing Wang^{b,d}

^aDepartment of Gastroenterology, Sir Run Run Shaw Hospital, School of Medicine, Zhejiang University, Zhejiang, China; ^bInstitute of Gastroenterology, Zhejiang University, Zhejiang, China; ^cDivision of Gastroenterology, Department of Internal Medicine, University of Michigan, Ann Arbor, MI, USA; ^dDepartment of Gastroenterology, Second Affiliated Hospital, Zhejiang University School of Medicine, Zhejiang, China; ^eDepartment of Cell Biology and Program in Molecular Cell Biology, Zhejiang University School of Medicine, Zhejiang, China

ABSTRACT

The enrichment of *Fusobacterium nucleatum* (*Fn*) has been identified in CRC patients and associated with worse outcomes. However, whether *Fn* was involved in the metastasis of CRC was not well determined. Here, we found that the abundance of *Fn* was significantly increased in CRC patients with lymph nodes metastasis. To further clarify the role of *Fn* in CRC metastasis, we performed transwell and wound healing assays after incubating CRC cell lines with or without *Fn* and injected *Fn*-treated or untreated CRC cells into nude mice via tail vein. The results indicated that *Fn* infection promoted CRC cells migration *in vitro*, as well as lung metastasis *in vivo*. Interestingly, colonization of *Fn* was detected in metastatic lung lesions of nude mice by fluorescence in situ hybridization. Mechanistically, RNA sequencing and validation study revealed that *Fn* significantly upregulated the expression of long non-coding RNA Keratin7-antisense (*KRT7-AS*) and Keratin7 (*KRT7*) in CRC cells. Importantly, *Fn*-induced CRC lung metastasis was attenuated by the depletion of *KRT7-AS*. In addition, *KRT7-AS* facilitated CRC cells migration by upregulating *KRT7*. Subsequently, we found that NF- κ B signaling pathway was involved in the upregulation of *KRT7-AS* upon *Fn* infection. In conclusion, *Fn* infection upregulated *KRT7-AS/KRT7* by activating NF- κ B pathway, which promoted CRC cell migration *in vitro* and metastasis *in vivo*.

ARTICLE HISTORY

Received 8 July 2019
Revised 8 November 2019
Accepted 16 November 2019

KEYWORDS

Fusobacterium nucleatum;
colorectal cancer;
metastasis; *KRT7-AS*; NF- κ B

Introduction

Colorectal cancer (CRC) is the fourth most common cancer and the second leading cause of cancer-related death worldwide.¹ Approximately 25% of patients with CRC show synchronous metastases while another 25% develop metastases throughout the course of their disease.² The prognosis of CRC patients with distant metastases is dismal with a 5-year survival rate of less than 10%.³ Unfortunately, the underlying mechanisms for the metastasis of CRC have not been fully clarified.

Recent evidence suggested that host–microflora interactions might play a key role in the initiation and progression of CRC. Study indicated that gavage of stool samples from patients with CRC promoted intestinal carcinogenesis in germ-free and conventional mice, which confirmed the

direct pro-tumorigenic effect of gut microbiota.⁴ Identification of specific carcinogenic microbiota remains an important area for CRC research. Previous studies have documented that several microbiota were involved in carcinogenesis of CRC, including *Peptostreptococcus anaerobius*,⁵ *enterotoxigenic Bacteroides fragilis*,⁶ *Escherichia coli*,⁷ and *Fusobacterium nucleatum* (*Fn*).⁸ However, previous studies mainly focused on the proliferative effects of microbiota, while their roles in the metastasis of CRC were not well explored.

Fn is a gram-negative anaerobic bacterium prevalent in the oral cavity which has gained significant attention for its potential role in CRC.^{9–12} The enrichment of *Fn* in CRC tissues compared to the adjacent normal tissues has been confirmed by several studies.^{11,13,14} Epithelial barrier defects

CONTACT Liangjing Wang ✉ wangljzju@zju.edu.cn Second Affiliated Hospital Zhejiang University, Hangzhou, China; Wei Zhuo ✉ 0012049@zju.edu.cn Department of Cell Biology and Program in Molecular Cell Biology Zhejiang University, Hangzhou, China; Jianmin Si ✉ sjm@zju.edu.cn Sir Run Run Shaw hospital Zhejiang University, Hangzhou, China

*These authors are considered to be joint first authors.

Supplemental data for this article can be accessed on the [publisher's website](#).

© 2020 Taylor & Francis Group, LLC

that occurred in sites of dysplasia might allow *Fn* to thrive in the local tumor environment.¹⁵ *Fn* possesses key pathogenic features that may allow it to predominate. Fap2, a surface protein of *Fn*, could bind to tumor-expressed Gal-GalNAc, which resulted in the enrichment of *Fn* in CRC.¹⁶ FadA, a unique virulence factor of *Fn*, could bind to E-cadherin and activate β -catenin, which stimulated tumor cell growth in CRC. Additionally, introduction of *Fn* to *Apc*^{Min/+} mice accelerated tumorigenesis.¹⁷ Furthermore, the presence of *Fn* might be a poor prognostic biomarker in CRC. The level of *Fn* DNA presented in CRC tissues was correlated with higher CRC-specific mortality.¹⁸ Meanwhile, *Fn* was associated with CRC recurrence and resistance to chemotherapy by activating the autophagy pathway.¹⁹

Recently, some clinical evidence suggested that the enrichment of *Fn* might be related to CRC metastasis.^{11,13,20–22} However, the role of *Fn* in CRC metastasis and its underlying mechanism remains unclear. This study first clarified the relationship between *Fn* infection and CRC metastasis. We found *Fn* infection upregulated *KRT7-AS/KRT7* by activating NF- κ B pathway, which promoted CRC cell migration *in vitro* and metastasis *in vivo*.

Results

Fn promoted CRC cells migration and metastasis

To identify the clinical significance of *Fn*, we performed qRT-PCR to quantify the abundance of *Fn* in fecal samples from CRC patients and healthy controls. The results indicated an enrichment of *Fusobacterium spp.* in the feces of CRC patients compared with healthy controls. Meanwhile, CRC patients with positive lymph nodes metastasis showed more abundance of *Fn* in feces compared to CRC patients without lymph nodes metastasis (Figure 1a). To evaluate the effect of *Fn* infection on CRC cell migration, we performed transwell and wound healing assays after incubating HCT-116 or LoVo cells with *Fn* for 12 h. The results indicated that *Fn* infection significantly enhanced HCT-116 and LoVo cells migration compared with *E. coli* DH5a or PBS control treatment (Figure 1b,c). However, heat-killed *Fn* was unable

to promote HCT-116 and LoVo cells migration (Supplementary Figure 1a,b). To confirm the results *in vitro*, we injected *Fn*-treated or PBS-treated HCT-116 cells into nude mice via tail vein. In accordance with the results *in vitro*, *Fn*-treated cells induced more metastatic nodules in lung than PBS-treated cells (Figure 1d). Notably, after intravenous injection of *Fn*-treated cells into nude mice, *Fn* was detected in the metastatic lung lesions by FISH assay (Figure 1e).

KRT7-AS/KRT7 expression is upregulated in *Fn*-treated CRC cells

Long-non-coding RNAs (*lncRNAs*) were reported to play essential roles in the metastasis of CRC.^{23,24} However, the interplay between *Fn* infection and *lncRNA* has never been identified. To explore whether *lncRNAs* were involved in *Fn* infection-induced CRC metastasis, we performed RNA sequencing to evaluate the expression profiles of *lncRNAs* after incubating LoVo cells with *Fn* or PBS for 24 h. The RNA sequencing results showed that *Fn* treatment significantly upregulated 43 *lncRNAs*, while downregulated 63 *lncRNAs* (FDR<0.05, $|\log_2$ (fold change)|>1) (Supplementary Table 1). Among these differentially expressed *lncRNA*, we were particularly interested in the *lncRNA Homo sapiens keratin 7 antisense RNA (KRT7-AS)*, which was one of the most differentially upregulated *lncRNAs* (FDR<0.0001, fold change = 6.06) (Figure 2a, Supplementary Figure 2). *KRT7-AS* was reported to be a single antisense RNA that was transcribed from the negative strand of the keratin 7 (*KRT7*) (Figure 2a).²⁵ Interestingly, RNA sequencing analysis also revealed that *KRT7* mRNA was consistently upregulated in *Fn*-treated cells (FDR<0.0001, fold change = 7.5) (Figure 2c). To validate RNA sequencing results, we performed qRT-PCR assay after incubating HCT-116 or LoVo cells with live or heat-killed *Fn*, *E.coli* or PBS control for 24 h. Consistently, both *KRT7-AS* and *KRT7* were significantly upregulated in live *Fn*-treated cells, while not in *E.coli* or heat-killed *Fn*-treated cells (Figure 2d). In addition, the expression of *KRT7-AS* and *KRT7* were simultaneously increased with the increasing *Fn*

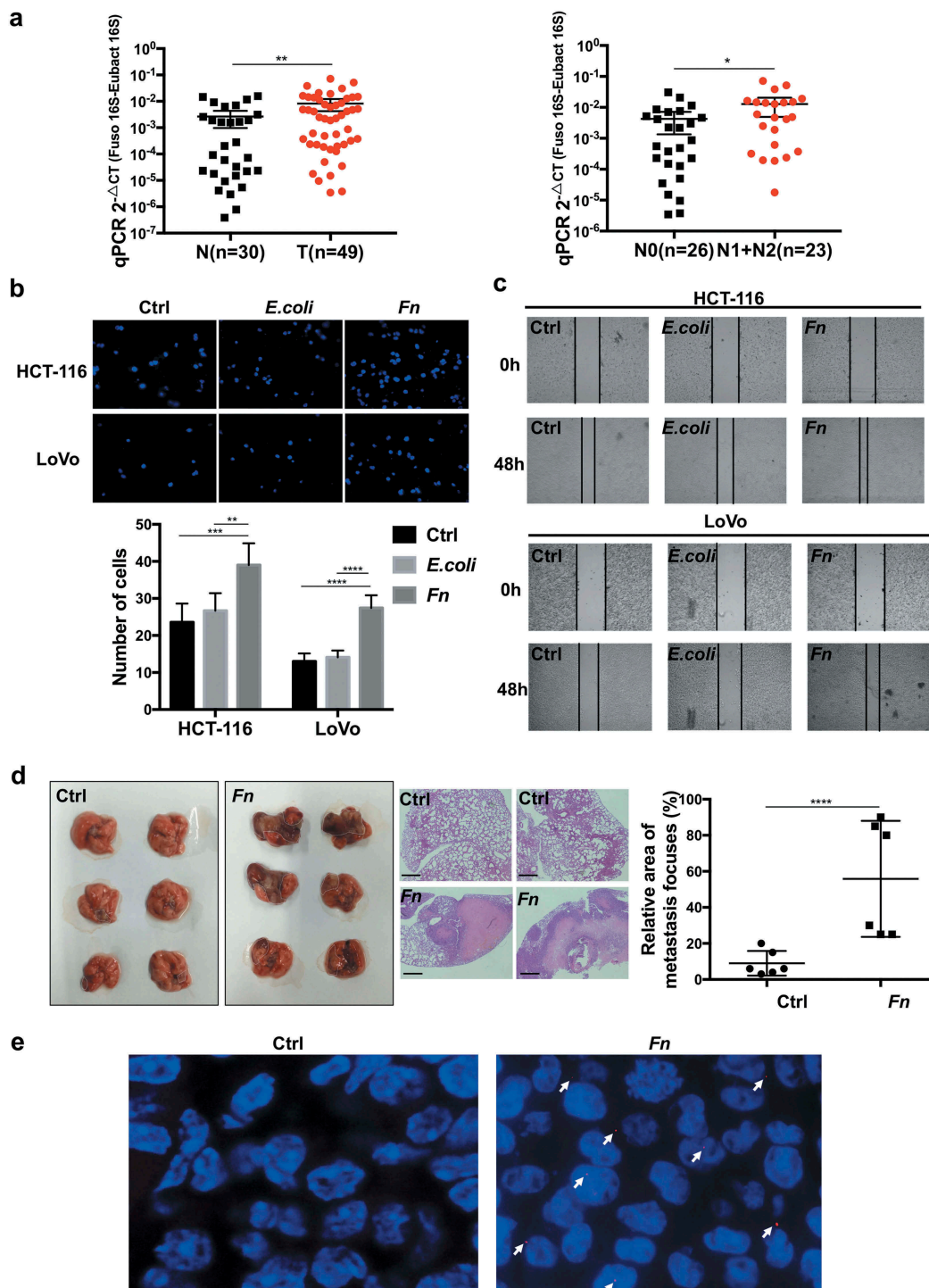


Figure 1. *Fn* promoted CRC cells migration and metastasis. (a) The abundance of *Fn* in the feces of CRC patients (T, n = 49) versus healthy people (N, n = 30). The abundance of *Fn* is higher in the feces of CRC patients with lymph nodes metastasis (N1+ N2, n = 23) than those without metastasis (N0, n = 26). (b,c) HCT-116 and LoVo cells were incubated with PBS control, *E. coli* or *Fn*. The migration ability of cells was evaluated by transwell assay (b) or wound healing assay (c). In transwell assay, migrated cells were stained with DAPI and images were randomly taken under microscope. Every 6 fields were counted for each sample. (d) HCT-116 cells were incubated with *Fn* or PBS for 24 h and then injected into BALB/C nude mice via tail vein (n = 6 per group). The left panel shows macroscopic lungs of nude mice. The area of metastatic lesions was labeled by dashed circles. The middle panel indicates the hematoxylin-eosin (H&E) staining of lung metastasis (scale bar = 100 μ m), two representative images per group. The right panel shows the statistical analysis of metastasis foci. (e) *Fn* in lung metastasis tissues was detected by FISH. The colonization of *Fn* was detected in lung metastasis from mice injected with *Fn*-treated cells (1000 times magnification power). The white arrows indicate positive stain. All data are shown as mean \pm SD, * p < .05, ** p < .01, *** p < .001, **** p < .0001 (Mann-Whitney test was used in a, unpaired Student's *t* test was used in b and d). Ctrl, control; *E. coli*, *Escherichia coli*; *Fn*, *Fusobacterium nucleatum*.

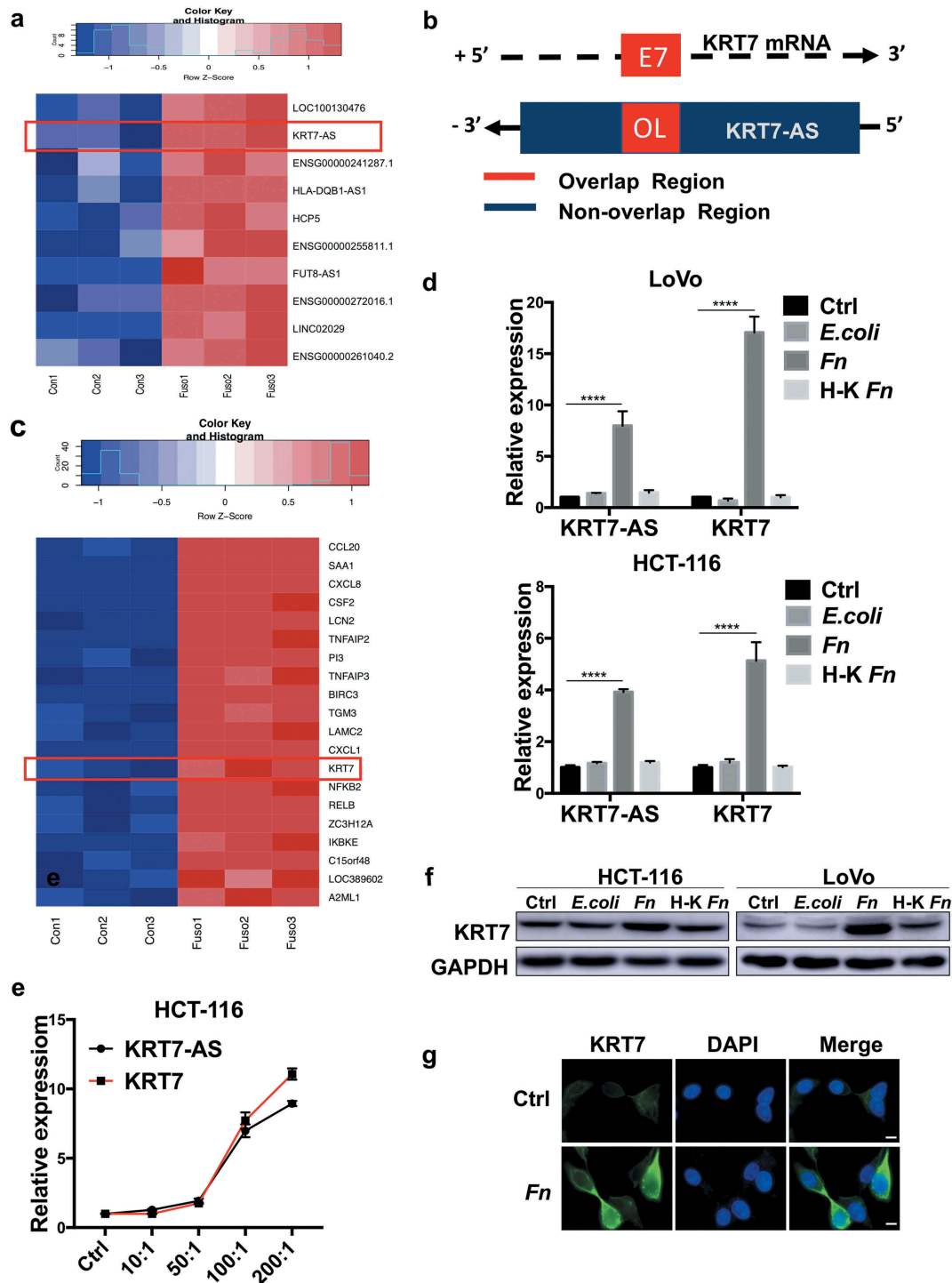


Figure 2. KRT7-AS/KRT7 expression is upregulated in *Fn*-treated CRC cells. (a) Heatmap of representative differentially expressed *lncRNA* between *Fn*-treated and PBS-treated LoVo cells ($n = 3$ per group, fold change > 2 , logCPM > 2 , FDR < 0.05). (b) The schematic representation of KRT7-AS (ensemble gene transcript ENST00000546688, on the negative DNA strand) and KRT7 mRNA (ReSeq gene NM_005556, on the positive strand). E7 indicates seventh exon of KRT7 gene. Black arrows indicates transcription direction. "+" indicates the positive strand. "-" indicates the negative strand. (c) Heatmap of representative differentially expressed mRNA between *Fn*-treated and PBS-treated cells ($n = 3$ each, fold change > 2 , logCPM > 2 , FDR < 0.05). (d) HCT-116 or LoVo were incubated with live or heat-killed *Fn*, *E.coli* or PBS for 24 h. The RNA expression level of KRT7-AS and KRT7 were analyzed by qRT-PCR. (e) HCT-116 cells were incubated with *Fn* in different multiplicity of infection (MOI) (10:1, 50:1, 100:1, 200:1) for 24 h and the expression level of KRT7-AS and KRT7 were analyzed by qRT-PCR. (f) HCT-116 or LoVo were incubated with live or heat-killed *Fn*, *E.coli* or PBS for 24 h. KRT7 protein was analyzed by Western blot. (g) HCT-116 were incubated with *Fn* or PBS for 24 h, immunofluorescence assay was conducted to show KRT7 protein in HCT-116 cells (scale bar = 50 μ m). All data are shown as mean \pm SD, **** $p < .0001$ (unpaired Student's *t* test). Ctrl, control; *Fn*, *Fusobacterium nucleatum*.

multiplicity of infection (MOI) (Figure 2e). We confirmed that *Fn* infection increased the protein levels of KRT7 by both Western blot and immunofluorescence assays (Figure 2f,g). Collectively, these results showed that *Fn* infection upregulated both *KRT7-AS* and KRT7 in CRC cells.

KRT7-AS promoted metastasis of CRC cells by regulating KRT7

To elucidate the interaction between *KRT7-AS* and KRT7, we then performed loss and gain of function assays in CRC cells. We found that knockdown of *KRT7-AS* in HCT-116 significantly suppressed mRNA and protein levels of KRT7 (Figure 3a,b). Meanwhile, overexpression of *KRT7-AS* in HCT-116 or LoVo cells upregulated the expression of KRT7 (Figure 3a,b, Supplementary Figure 3a). In contrast, knockdown or overexpression of KRT7 had no effect on the expression of *KRT7-AS* (Figure 3a,b, Supplementary Figure 3a,b).

Then, we performed wound healing and transwell assays to evaluate the role of *KRT7-AS* and KRT7 in CRC cell migration. Knockdown of *KRT7-AS* or KRT7 in HCT-116 significantly inhibited cell migration, while overexpression of *KRT7-AS* or KRT7 in HCT-116 or LoVo promoted cell migration (Figure 3c,d, Supplementary Figure 3c). To confirm the function of *KRT7-AS* *in vitro*, we stably transfected HCT-116 cells with *KRT7-AS* shRNA or control lentivirus and then injected these infected cells into nude mice. Result indicated knockdown of *KRT7-AS* significantly inhibited lung metastasis of nude mice (Figure 3e, Supplementary Figure 3d). In addition, overexpression of KRT7 restored the suppressed migration properties of HCT-116 cells induced by knockdown of *KRT7-AS* (Figure 3f). These results indicated that *KRT7-AS* promoted metastasis of CRC cells by upregulating KRT7.

Fn promoted metastasis of CRC by modulating KRT7-AS/KRT7

To determine whether the effect of *Fn* on the metastasis of CRC cells was mediated by *KRT7-AS/KRT7*, we treated HCT-116 cells with siRNA targeting *KRT7-AS* alone or together with *Fn*. We observed that knockdown of *KRT7-AS* attenuated

Fn-induced upregulation of KRT7 (Figure 4a,b). The pro-migratory effect induced by *Fn* infection was abolished by knockdown of *KRT7-AS* or KRT7 in HCT116 cells (Figure 4c). To confirm these results *in vitro*, HCT-116 cells which were stably transfected with *KRT7-AS* shRNA or control lentivirus were incubated with *Fn* or PBS for 24 h and then injected into nude mice. Consistent with above result, *Fn* treatment significantly induced more lung metastatic nodules. Importantly, depletion of *KRT7-AS* attenuated *Fn*-induced CRC lung metastasis (Figure 4d). These results suggested that *Fn* promoted metastasis of CRC cells by upregulating the expression of *KRT7-AS/KRT7*.

Fn regulated KRT7-AS through NF-κB signaling pathway

The mechanism for the upregulation of *KRT7-AS* upon *Fn* infection remained unclear. Therefore, we aimed to find certain pathway regulated by *Fn* and identify the upstream regulators of *KRT7-AS*. KEGG analysis based on RNA sequencing results demonstrated that NF-κB pathway was activated by *Fn* infection (Figure 5a). We validated this result by performing Western blot after incubating HCT-116 or LoVo cells with live or heat-killed *Fn*, *E.coli* or PBS control for 24 h. Consistently, live *Fn* treatment dramatically upregulated phospho-p65 (activated NF-κB subunit), and downregulated IκB-α (NF-κB inhibitor) compared with heat-killed *Fn*, *E.coli* or PBS control (Figure 5b). Similarly, we observed increased nuclear localization of NF-κB p65 in *Fn*-treated CRC cells (Figure 5c).

We next used two software packages (TESS and FIMO)^{26,27} to predict transcriptional factor binding to the promotor region of *KRT7-AS*. Interestingly, the consensus binding sequence (−2470–2461 bp 5′-GGGAACCCCA-3′) for NF-κB p65 in the promotor region of *KRT7-AS* was predicted. Knockdown of NF-κB p65 in HCT-116 or LoVo significantly decreased the expression of *KRT7-AS* as well as KRT7 (Figure 5d,e, Supplementary Figure 3e). Administration with an NF-κB inhibitor, BAY-117082, at different concentrations to HCT-116 cells also significantly decreased expression of *KRT7-AS* and KRT7 (Figure 5f, Supplementary Figure 3f). In addition,

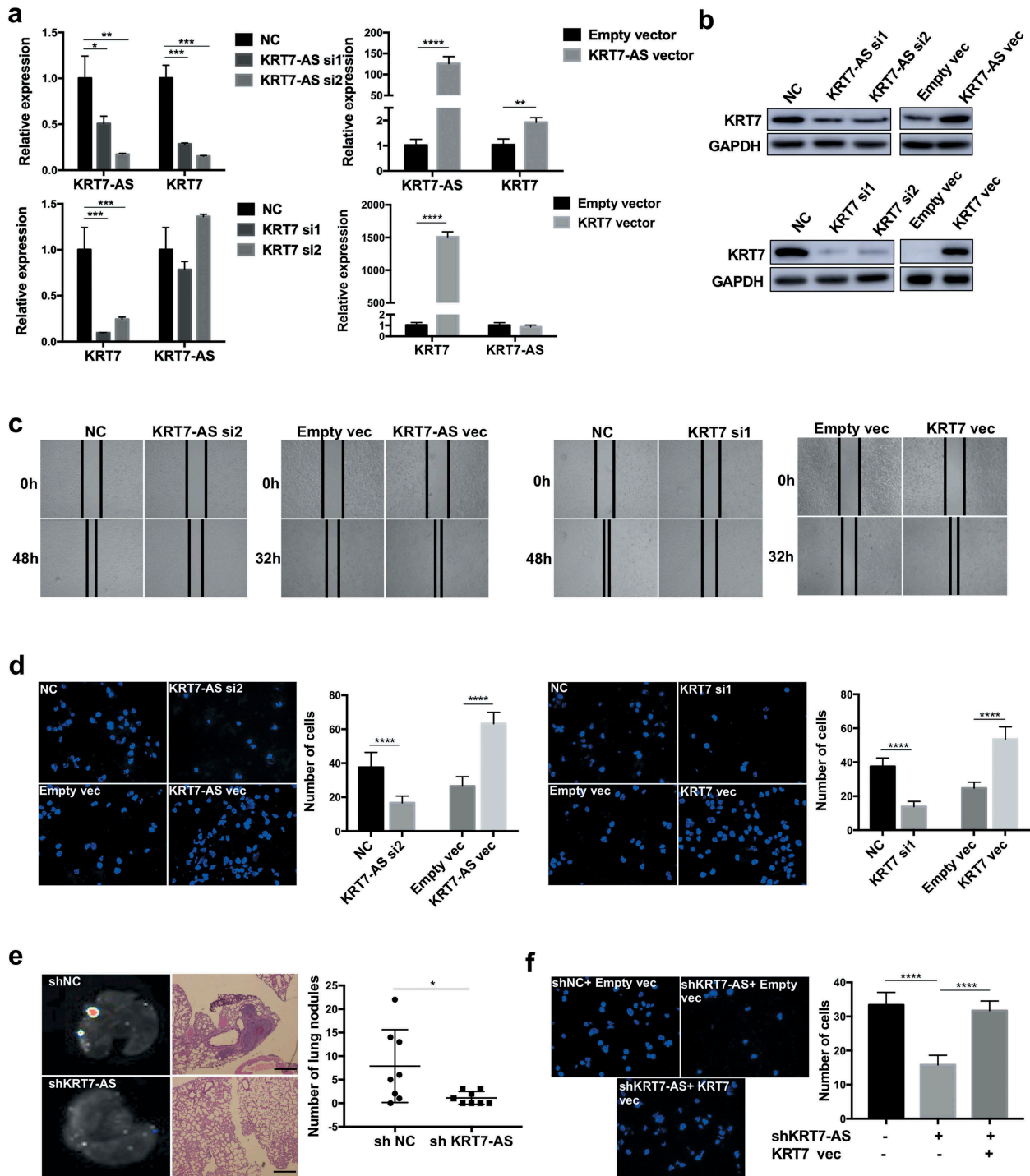


Figure 3. *KRT7-AS* promoted metastasis of CRC cells by regulating *KRT7*. (a) RNA level of *KRT7-AS* and *KRT7* was detected by qRT-PCR after knockdown of *KRT7-AS* (upper left panel) or overexpression of *KRT7-AS* (upper right panel), respectively, in HCT-116 cells. Expression level of *KRT7-AS* and *KRT7* were detected by qRT-PCR after knockdown of *KRT7* (lower left panel) or overexpression of *KRT7* (lower right panel), respectively, in HCT-116 cells. (b) *KRT7* protein level was detected by Western blot after knockdown or overexpression of *KRT7-AS* or *KRT7*. (c, d) HCT-116 cells were transfected with siRNA targeting *KRT7-AS* (*KRT7*) or *KRT7-AS* (*KRT7*) plasmids. Wound healing assays (c) and transwell assays (d) were performed. For transwell assay, migrated cells were stained with DAPI and images were randomly taken under microscope. Every 6 fields were counted for each sample. (e) HCT-116 cells stably transfected with *KRT7-AS* shRNA lentivirus were established and injected into nude mice via tail vein. The number of metastatic nodules in each slide was counted after H&E staining. (n = 8 mice per group). GFP signal shows metastatic cells infected by lentivirus in lungs. (f) HCT-116 cells were transfected with sh*KRT7-AS* lentivirus alone or combined with *KRT7* overexpression plasmid, and transwell assay was performed. Migrated cells were stained with DAPI and images were randomly taken under microscope. Every 6 fields were counted for each sample. All data are shown as mean \pm SD, * $p < .05$, ** $p < .01$, *** $p < .001$, **** $p < .0001$ (unpaired Student's *t* test). NC, negative control; *Fn*, *Fusobacterium nucleatum*; vec, vector; si, siRNA.

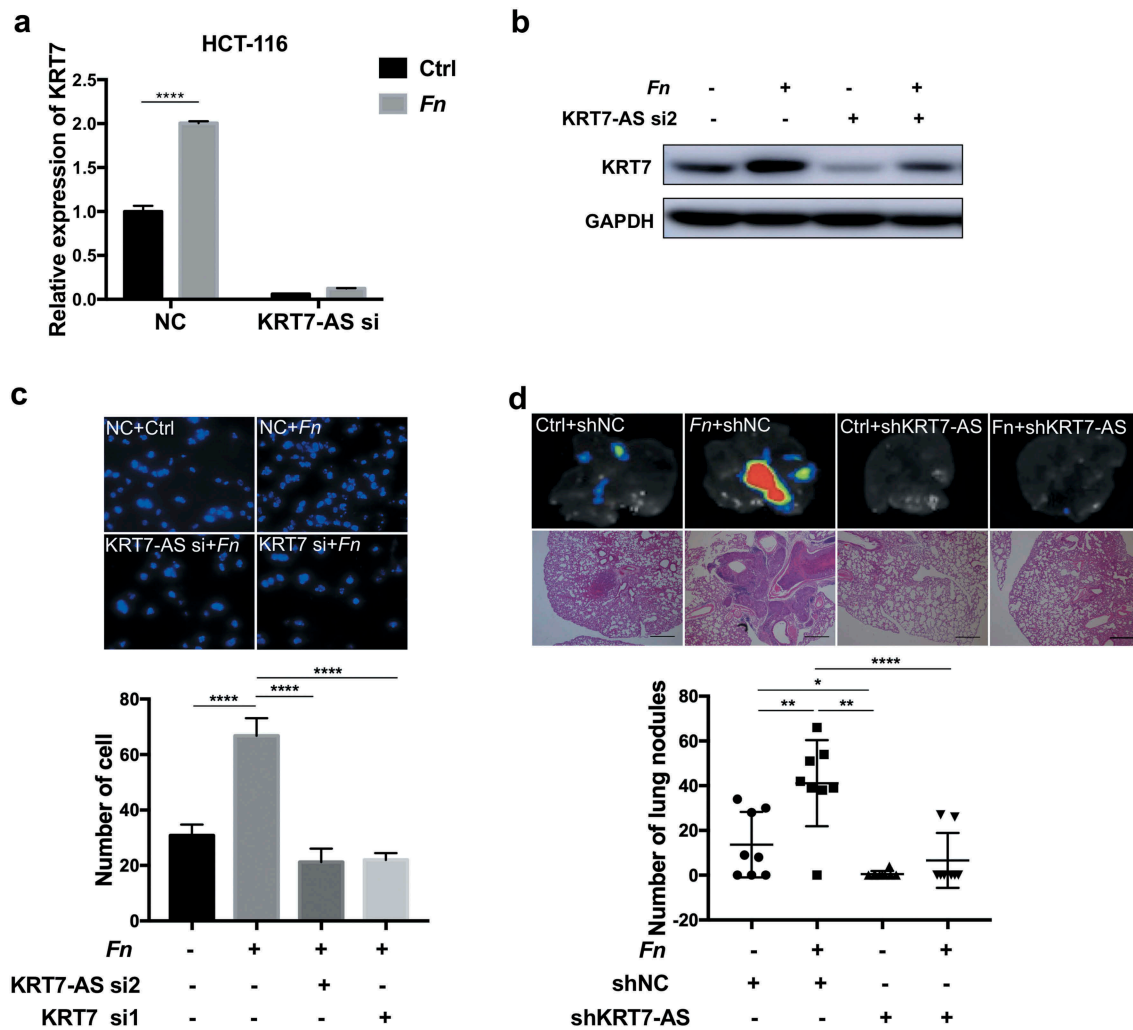


Figure 4. *Fn* promoted metastasis of CRC by modulating *KRT7-AS/KRT7*. (a,b) HCT-116 cells were transfected with siRNA targeting *KRT7-AS* and then incubated with *Fn*. qRT-PCR (a) and western blot (b) indicated that knockdown of *KRT7-AS* suppressed the *Fn*-induced upregulation of KRT7. (c) HCT-116 cells were transfected with siRNA targeting *KRT7-AS* or KRT7 and then incubated with *Fn* or PBS. Transwell assay was performed. Migrated cells were stained with DAPI and images were randomly taken under microscope. Every 6 fields were counted for each sample. (d) HCT-116 cells were stably transfected with *KRT7-AS* shRNA or control lentivirus and then incubated with *Fn* or PBS for 24 h. Then, above-prepared cells were injected into nude mice via tail vein ($n = 8$ each group). The number of metastatic nodules in lung was counted in each slide after H&E staining (scale bar = 100 μ m). GFP signal shows metastatic HCT-116 cells infected by lentivirus in lungs. All data are shown as mean \pm SD, * $p < .05$, ** $p < .01$, **** $p < .0001$ (unpaired Student's t-test). NC, negative control; *Fn*, *Fusobacterium nucleatum*; si, siRNA.

the upregulation of *KRT7-AS* by *Fn* infection was attenuated when HCT-116 cells were pretreated with NF- κ B inhibitor, BAY-117082 (Figure 5f). Next, we constructed luciferase reporter plasmid containing promoter region of *KRT7-AS* to determine the interaction between p65 and *KRT7-AS* promoter. The luciferase reporter assay showed that knockdown of p65 significantly decreased the transcriptional activity of *KRT7-AS* (Figure 5g). These results demonstrated that *Fn* infection increased *KRT7-AS* expression through activating NF- κ B signaling pathway.

The expression of *KRT7-AS/KRT7* in CRC patients

To identify the clinical significance of *KRT7-AS* and KRT7, we performed qRT-PCR to quantify the expression of *KRT7-AS* and KRT7 using fresh frozen tissues from CRC patients. The expression of *KRT7-AS* and KRT7 was significantly increased in CRC tissues compared with adjacent normal tissues ($n = 83$) (Figure 6a). Consistently published data from The Cancer Genome Atlas (TCGA) also demonstrated that *KRT7-AS* and KRT7 expression were significantly elevated in colon cancer tissues

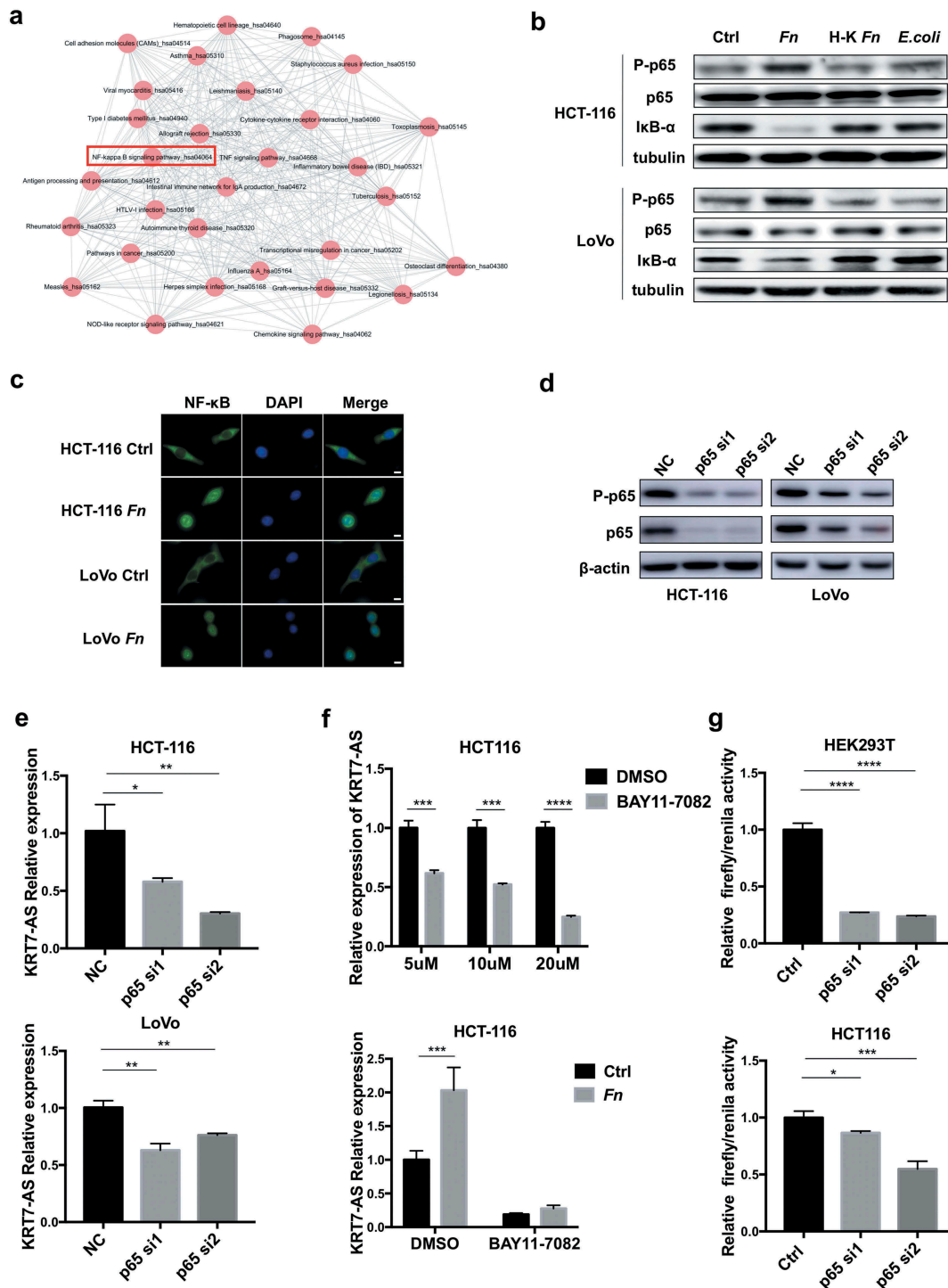


Figure 5. *Fn* regulated *KRT7-AS* through NF-κB signaling pathway. (a) The KEGG analysis based on RNA sequencing result shows activation of NF-κB induced by *Fn* infection. (b) HCT-116 or LoVo cells were incubated with live or heat-killed *Fn*, *E.coli* or PBS for 24 h. The protein level of phospho-p65, p65, and IκB-α was measured by Western blot. (c) HCT-116 or LoVo were incubated with *Fn* or PBS control for 2 h. Immunofluorescence assay was performed to detect the p65 in the nucleus. DAPI was used to stain cell nucleus (scale bar = 50 μm). (d) Western blot shows the efficiency of two siRNA targeting p65. (e) HCT116 or LoVo was transfected with siRNA targeting p65. After 48 h, the qRT-PCR was performed to analyze the expression of *KRT7-AS*. (f) HCT-116 cells were treated with BAY-117082 (Selleck, USA) in different concentrations (5 μM, 10 μM, 20 μM) for 2 h (upper panel). HCT-116 cells were treated with 20 μM BAY-117082 for 2 h followed by *Fn* incubation for 4 h (lower panel). The qRT-PCR was performed to analyze the expression of *KRT7-AS*. (g) HEK293T and HCT-116 cells were transfected with luciferase reporter plasmid along with p65 siRNA or negative control. After 48 h, the luciferase activity was measured. The transfection efficiency data were normalized by dividing the Firefly luciferase activities with that of Renilla luciferase. All data are shown as mean ± SD, **p* < .05, ***p* < .01, ****p* < .001, *****p* < .0001 (unpaired Student's *t*-test). Ctrl, control; NC, negative control; *Fn*, *Fusobacterium nucleatum*; si, siRNA.

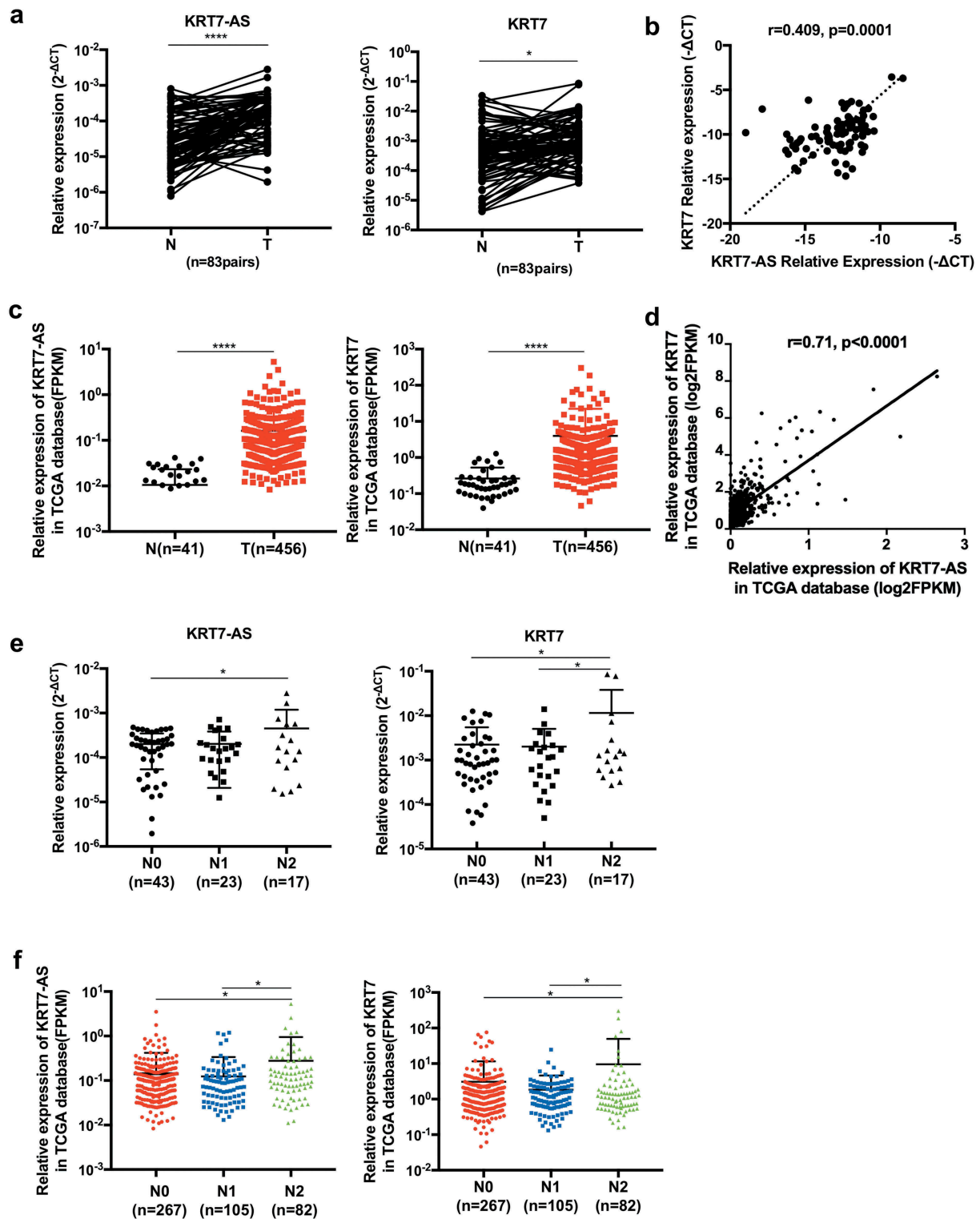


Figure 6. The expression of KRT7-AS/KRT7 in CRC patients. (a) The qRT-PCR analysis of the expression of KRT7-AS and KRT7 in CRC tissues and their adjacent normal tissues (n = 83 pairs). (b) Correlation analysis of the expression of KRT7-AS with KRT7 in our tested CRC tissues (n = 83, spearman $r = 0.409$, $p < .0001$). (c) Data in TCGA database showed the expression levels of KRT7-AS and KRT7 in colon cancer compared with those of normal controls (n = 456 vs. 41). (d) Correlation analysis of the expression of KRT7-AS with KRT7 in TCGA database (n = 456, spearman $r = 0.71$, $p < .0001$). (e, f) The expression of KRT7-AS and KRT7 among CRC patients with different N stage (N0, N1, N2) in our tested CRC tissue (e) and TCGA database (f). All data are shown as mean \pm SD, * $p < .05$, ** $p < .01$, *** $p < .001$, **** $p < .0001$ (Wilcoxon matched-pairs signed-rank test was used in a, Mann-Whitney test was used in c, spearman correlation analysis was used in b and d, one-way ANOVA was used in e and f). *Fn*, *Fusobacterium nucleatum*.

compared with normal tissues (Figure 6c). Furthermore, the *KRT7-AS* expression was positively associated with *KRT7* expression both in our tested CRC tissues and TCGA database (Figure 6b, d). Though the expression of *KRT7-AS* and *KRT7* were not increased in N1 patients compared with N0 patients, both our tested CRC tissues and TCGA database consistently showed that the expression of *KRT7-AS* and *KRT7* were significantly increased in CRC tissue of N2 patients. These results indicated that both *KRT7-AS* and *KRT7* were positively associated with more advanced N stage in CRC patients (Figure 6e,f).

Discussion

In the present study, we observed that the abundance of *Fn* was significantly increased in CRC patients with lymph nodes metastasis than those without lymph nodes metastasis. Furthermore, we reported that *Fn* infection enhanced CRC cells migration *in vitro* and increased lung metastasis *in vivo*. Several previous studies also indicated that the abundance of *Fn* was associated with TNM stage and survival outcomes in CRC patients.^{11,13,18,20,21} Interestingly, Bullman *et al.* recently found identical *Fusobacterium* strains in human primary CRC tissues and paired metastatic tumors in liver, suggesting these bacteria may migrate with colorectal cancer cells to distant sites.²² Inconsistent with this assumption, we also found the existence of *Fn* in metastatic lung lesions from mice which were intravenously injected with *Fn*-treated cells. These findings indicated that *Fn* not only plays a pro-tumorigenic role in CRC but also promotes distant metastasis.

The mechanisms for pro-metastatic effect upon *Fn* infection are not fully understood. Long-non-coding RNAs (*lncRNAs*) were reported to play essential roles in the metastasis of CRC.^{23,24} The crosstalk between *Fn* and *lncRNA* has never been clarified. We hypothesized that *lncRNA* might be involved in the progression of CRC upon *Fn* infection. Interestingly, we discovered a great number of differentially expressed *lncRNAs* induced by *Fn* infection, among which *KRT7-AS* is one of the most differentially upregulated *lncRNA*. Prior study has demonstrated that overexpression of *KRT7-AS* in gastric cancer cells promoted cell

growth, S-phase entry, and migration.²⁵ However, its role in CRC was unknown. We found that *KRT7-AS* was associated with advanced N stage and *Fn* infection promoted CRC metastasis in a *KRT7-AS* dependent manner.

Previous study indicated that *KRT7-AS* upregulated protein and mRNA levels of *KRT7* by stabilizing *KRT7* mRNA in gastric cancer.²⁵ In our study, we also found the similar interaction between *KRT7-AS* and *KRT7* in CRC cells. *KRT7* belongs to type II cytokeratin, which is the component of cytoskeleton and epithelial intermediate filaments.^{28,29} In addition to its role in maintaining the structural integrity of the cells, intermediate filaments, such as *KRT7*, have interesting properties that may promote motile activities.³⁰ *KRT7* was expressed in approximately 10% of all colorectal tumors and associated with high extent of tumor budding and worse outcomes.³¹ Reyhan *et al.* demonstrated that *KRT7* expression was more common in CRC with lymph nodes metastasis compared to those without lymph nodes metastasis.³² Though *KRT7* overexpression has been observed in CRC, the biological significance is unknown.^{25,31} We found that *KRT7* was a downstream target of *KRT7-AS* and could regulate the migration of CRC cells. In this study, we attempted to clarify the mechanism for the upregulation of *KRT7-AS* by *Fn* infection. We found that *Fn* infection activated NF- κ B pathway. The activated NF- κ B *P*-p65 might upregulated *KRT7-AS* by enhancing the transcriptional activity of *KRT7-AS*.

In conclusion, our study confirmed an association between *Fn* and CRC metastasis and uncovered a novel mechanism by which *Fn* promoted CRC metastasis. This raises important questions on whether the depletion of *Fn* can prevent the early-stage CRC patients from an exacerbation and whether treatment regimens should be tailored based on the presence or absence of *Fn* in the metastatic spread of CRC patients.

Materials and methods

Bacterial strain and cell culture

Fn was purchased from American type culture collection (ATCC, *Fusobacterium nucleatum* subsp. *nucleatum* ATCC 25586). *Fn* was grown in Columbia blood agar

(bioMerieux Biotech Co., Shanghai, China) in an anaerobic jar (MITSUBISHI Gas Chemical Co., Japan) at 37°C. Heat-killed *Fn* was prepared by heating the bacteria at 95°C for 1 h. The *E. coli* strain DH5a (Takara, Japan) was cultured in Luria-Bertani medium. CRC cell lines (HCT-116, LoVo) were purchased from ATCC. HCT-116 were cultured in Maccoy 5A (Genom, China) supplemented with 10% fetal bovine serum (FBS), while LoVo was cultured in F-12K (Genom, China) supplemented with 10% FBS. All CRC cell lines were cultured at 37°C in humidified 5% CO₂ atmosphere.

Patients and public involvement

Fecal samples were collected from 49 previously untreated CRC patients and 30 healthy people from Sir Run Run Shaw Hospital, Zhejiang University School of Medicine. Fresh cancer and adjacent normal tissues were obtained from 83 CRC patients. In addition, published data of 456 colon carcinomas (with 41 normal tissues) from The Cancer Genome Atlas (TCGA) were analyzed. Written informed consents were obtained from all participants. The study was approved by the Institutional Review Board of Sir Run Run Shaw hospital.

RNA extraction and quantitative real-time PCR

Total RNAs were extracted from CRC cell lines or fresh frozen tissues using Trizol reagent (Ambion, USA). 1 µg of total RNAs were reverse transcribed to cDNA using PrimeScript RT Reagent Kit (Takara, Japan). Quantitative real-time PCR was performed in ROCHE LightCycler®480 System (Rotor gene 6000 Software, Sydney, Australia). Each reaction was assayed in triplicate in 10 µl reactions containing SYBR Premix Ex Taq (Takara, Japan), primers and template DNA. The Ct values obtained from samples were compared using 2^{-ΔΔCt} method. *GAPDH* or *U6* served as internal reference genes. The following primer sets were used:

KRT7-AS-F, 5'-TCCAACGCCTATGTTCCAGTTC-3',
KRT7-AS-R, 5'-ACATTGTGCCACGGACATCTTG-3';²⁵
KRT7-F, 5'-CGGCATCATCGCTGAGGTCAA-3',
KRT7-R, 5'-GCCTGGAGGGTCTCAAACCTTG-3';²⁵

U6-F, 5'-CTCGCTTC-GGCAGCACA-3',
U6-R, 5'-AACGCTTCACGAATTTGCGT-3';
GAPDH-F, 5'-GCACCGTCAAGGCTGAGAA-3',
GAPDH-R, 5'-TGGTGAAGACGCCAGTGGA-3'.

Fn quantification

Fn quantification was performed as described previously.^{17,19} DNA from fecal samples were extracted using QIAGEN stool kit (QIAGEN, Germany). *Fn* quantification was performed by real-time PCR. Relative abundance was calculated by 2^{-ΔCt} method. Universal Eubacteria 16s was used as reference gene. The following primer sets were used:

Fusobacterium spp-F, 5'-CGGGTGAGTAACGCGTAAAG-3',
Fusobacterium spp-R, 5'-ACATTGTGCCACGGACATCTTG-3';³³
 universal Eubacteria 16s-F, 5'-CGGCAACGAGCGCAACCC-3',
 universal Eubacteria 16s-R, 5'-CCATTGTAGCACGTGTGTAGCC-3'.³⁴

Western blotting

Total proteins were extracted from CRC cell lines or fresh frozen tissues using RIPA lysis buffer and quantified using BCA Protein Assay Kit (Beyotime, China). Protein was electrophoresed through 10% SDS polyacrylamide gels and then transferred to PVDF membranes. The membranes were blocked with 5% fat-free milk for 2 h and incubated with primary antibodies at 4°C overnight. The following primary antibodies were used: KRT7 (1:1000 CST#4466), p65 (1:1000 CST#8242), P-p65 (1:1000 CST#3033) and IκB-α (1:1000 CST#9294). Membranes were then incubated with second antibodies labeled with HRP at room temperature on the following day and the signal was detected using an ECL kit (Fdbio science, China). *GAPDH* was used as a reference gene.

Immunofluorescence (IF)

CRC cells were seeded on chamber slides and then fixed with 4% paraformaldehyde for 10 min. The slides were incubated with 0.2% TritonX-100 (Beyotime, China) for 15 min and blocked in 3%

BSA for 0.5 h. After washing by PBS for three times, the cells were incubated with primary antibodies against KRT7 (1:100 CST#4465) or NF- κ B (1:400, CST #8242) at 4°C overnight in wet chamber. On the following day, the slides were washed by PBST for three times and incubated with secondary antibodies at room temperature for 1 h. The cells were then stained with DAPI.

Transwell migration assays

CRC cells were incubated with *Fn* or *E. coli* DH5a at multiplicity of infection (MOI) of 100:1 for 12 h. Cells treated with PBS were set as negative control. The infected cells were resuspended in 200 μ l medium without serum and were seeded into upper chambers of transwell chambers (Corning, USA) while lower chambers were filled with medium containing 10% FBS. After 20 h, the cells remaining in the upper chamber were removed while cells that had migrated across the transwell membrane were stained with DAPI. Images were randomly taken under fluorescence microscope. Every 6 fields were counted for each sample.

Wound healing assays

CRC cells were seeded in 6-well plates and left to grow until confluent. After wounding with yellow pipette tips, the cells of each well were incubated with *Fn* or *E. coli* DH5a at MOI of 100:1. Cell images were taken at 6, 24, 36 and 48 h, respectively.

Small interfering RNAs (siRNAs), lentivirus shRNA and plasmid

Two different siRNAs which exclusively targeted KRT7-AS RNA

(siRNA1, 5'-CUGAAUGUGUGCTGAGGAUCAA
ATT-3';

siRNA2, 5'-GAGGAUGAAAUGAGAUAAUT
T-3')²⁵

and siRNAs targeted against KRT7 mRNA non-overlapping region

(siRNA1, 5'-UGGAGGACUUCAAGAAUAAT
T-3';

siRNA2, 5'-ACAAGCUGCUGGAGACCAATT-
3')²⁵

were used. In addition, two different siRNA were used to target NF- κ B p65

(siRNA1, 5'-GCTGATGTGCACCGACAAGT
T-3';

siRNA2, CAGAUACAGACGAUCGUCATT).

A non-targeting sequence (5'-UUCUCCGAACGUGUCACGUTT-3') was used as negative control (NC). All siRNAs were synthesized by GenePharma Co. China. Lentivirus shRNAs were constructed by Genechem Co. China. Briefly, the siRNA targeting KRT7-AS (5'-GAGGATGAAATGAGATAAT-3') was synthesized and a non-targeting sequence 5'-TTCTCCGAACGTGTCACGT-3' was set as negative control (NC). The DNA fragments containing loop-structure for specific short-hairpin RNA were cloned into GV248 (hU6-MCS-Ubiquitin-EGFP-IRES-puromycin). KRT7-AS and KRT7 overexpression plasmids were constructed by Genechem Co. China. Genes were cloned into pCDNA 3.1(+).

Cell transfection

The siRNAs were transfected into cells using Lipofectamine[™] RNAiMAX (Thermo Fisher Scientific, Massachusetts, USA) in opti-MEM (Genom, China) according to the manufacturer's protocol. Plasmids were transfected into cells using FuGENE HD transfection reagent (Promega, USA) in opti-MEM according to the manufacturer's protocol.

RNA sequencing

LoVo cells were incubated with *Fn* (MOI = 100:1) or PBS for 24 h. Total RNAs were extracted from LoVo treated by *Fn* or PBS using Trizol reagent, and ribosomal RNA was removed using the Ribo-Zero[™] kit (Epicenter, Madison, WI, USA). Subsequently, the purified RNAs were subjected to first strand and second strand cDNA synthesis followed by adaptor ligation and enrichment with a low-cycle according to instructions of NEBNext[®] Ultra[™] RNA Library Prep Kit for Illumina (San Diego, CA, USA). The purified library products

were evaluated using the Agilent 2200 TapeStation and Qubit®2.0 (Life Technologies, USA). The libraries were paired-end sequenced (PE150, Sequencing reads were 150 bp) at Guangzhou RiboBio Co., Ltd. (China) using Illumina HiSeq 3000 platform. Raw fastq sequences were treated with Trimmomatic tools (v 0.36) to remove trailing sequences below a phred quality score of 20 and to achieve uniform sequence lengths for downstream clustering processes. Paired-end reads were aligned to the mouse reference genome mm10 and reads numbers mapped to each gene were counted by using Gfold (V1.1.2). The whole samples expression levels were presented as RPKM (expected number of Reads PerKilobase of transcript sequence per Million base pairs sequenced). The statistically significant differentially expressed genes were obtained by an adjusted *p*-value threshold of <0.05 and $|\log_2(\text{fold change})| > 1$ using the edgeR (v 3.10.0) software. All the *p*-values were adjusted by FDR (False discovery rate) in multiple comparisons. To look for meaningful *Fn*-targeted lncRNA and mRNA, we filtered out lncRNA and mRNA with very low expression level ($\log\text{CPM} < 2$) among all the differentially expressed lncRNA and mRNA and obtained top 10 upregulated lncRNA and top 20 upregulated mRNA to do heatmap. All differentially expressed genes were used for KEGG ontology enrichment analyses. For KEGG enrichment analysis, a *p* value < 0.05 was used as the threshold to determine the significant enrichment of the gene sets. All differentially expressed lncRNA and mRNA list as well as KEGG pathways were shown in Supplementary Tables 1–3.

Lung metastasis in vivo

BALB/c female nude mice aged 5 weeks were purchased from Shanghai SLAC Laboratory Animal Co. China. HCT-116 cells were incubated with *Fn* at MOI of 100:1 for 24 h. Cell resuspension solutions were injected via tail vein, 10^6 cells in 100 μl per mouse. Two months later, the mice were sacrificed and their lungs were surgically excised, photographed, and measured. Subsequently, lung tissues were fixed in 10% formalin and embedded in paraffin for hematoxylin and eosin (H&E) staining to confirm histology. All nude mice were raised in a specific-pathogen-free

condition. All animal procedures were performed in compliance with ethical standards and approved by the Animal Care Committee of Zhejiang University.

Fluorescence In Situ Hybridization (FISH)

Detection of *Fn* was performed by FISH on formalin-fixed paraffin-embedded (FFPE) section of lungs tissue from nude mice as described previously.^{35,36} The sequence of *Fn* targeted probe (5'-CGCAATACAGAGTTGAGCCCTGC-3')¹¹ was synthesized by Guangzhou EXON Biological Technology Co. China.

Luciferase reporter assay

The DNA fragment of *KRT7-AS* promotor was amplified and cloned into the pGL3-Enhancer Vector (Taihe Biotechnology Co. China). The reporter plasmid was co-transfected with p65 siRNA or negative control siRNA into HEK293T or HCT-116 cells. Luciferase assays were performed 48 h after transfection by using Dual-Luciferase Reporter Assay System (Promega). Renilla luciferase activity was used as a reference. The transfection efficiency data were normalized by dividing the Firefly luciferase activities with that of Renilla luciferase.

Statistical analysis

Experimental results were evaluated using paired or unpaired Student's t-test for normally distributed data and Mann-Whitney U test or Wilcoxon Sign-Rank test for non-parametric data. One-way ANOVA and Tukey's multiple comparison were used for test among three groups. The Correlation analysis was performed using Spearman rank correlation test. Data were shown as mean \pm standard deviation (SD). All *p* values were two-tailed and *p* values less than 0.05 were considered statistically significant. All statistical analyses were conducted using SPSS 22.0 or GraphPad Prism 7.

Disclosure of potential conflicts of interest

No potential conflicts of interest were disclosed.





Authors' contributions

Li.W., J.S. and W.Z. designed the experiment and supervised the study. T.S. and S.C. performed the experiments, analyzed the data and wrote the manuscript. Y.Z., J.H., Q.G., and L. W. performed the experiments. Li.W. and A.L. reviewed and revised the manuscript.

Funding

This work was supported by National Key R&D Program of China [2016YFC1303200] and the National Natural Science Foundation of China [81702308, 81972276].

ORCID

Allen Lee  <http://orcid.org/0000-0002-4861-7646>
 Qiwei Ge  <http://orcid.org/0000-0003-1689-6836>
 Wei Zhuo  <http://orcid.org/0000-0002-8251-4210>
 Liangjing Wang  <http://orcid.org/0000-0001-8227-8855>

References

- Bray F, Ferlay J, Soerjomataram I, Siegel RL, Torre LA, Jemal A. Global cancer statistics 2018: GLOBOCAN estimates of incidence and mortality worldwide for 36 cancers in 185 countries. *CA Cancer J Clin.* 2018;68:394–424. doi:10.3322/caac.21492.
- Bruckner HW, Motwani BT. Chemotherapy of advanced cancer of the colon and rectum. *Semin Oncol.* 1991;18:443–461.
- Dahan L, Sadok A, Formento JL, Seitz JF, Kovacic H. Modulation of cellular redox state underlies antagonism between oxaliplatin and cetuximab in human colorectal cancer cell lines. *Br J Pharmacol.* 2009;158(2):610–620. doi:10.1111/j.1476-5381.2009.00341.x.
- Wong SH, Zhao L, Zhang X, Nakatsu G, Han J, Xu W, Xiao X, Kwong TNY, Tsoi H, Wu WKK, et al. Gavage of fecal samples from patients with colorectal cancer promotes intestinal carcinogenesis in germ-free and conventional mice. *Gastroenterology.* 2017;153(6):1621–33 e6. doi:10.1053/j.gastro.2017.08.022.
- Tsoi H, Chu ESH, Zhang X, Sheng J, Nakatsu G, Ng SC, Chan AWH, Chan FKL, Sung JJY, Yu J. *Peptostreptococcus anaerobius* induces intracellular cholesterol biosynthesis in colon cells to induce proliferation and causes dysplasia in mice. *Gastroenterology.* 2017;152(6):1419–33 e5. doi:10.1053/j.gastro.2017.01.009.
- Thiele Orberg E, Fan H, Tam AJ, Dejea CM, Destefano Shields CE, Wu S, Chung L, Finard BB, Wu X, Fathi P, et al. The myeloid immune signature of enterotoxigenic *Bacteroides fragilis*-induced murine colon tumorigenesis. *Mucosal Immunol.* 2017;10(2):421–433. doi:10.1038/mi.2016.53.
- Zhang S, Fu J, Dogan B, Scherl EJ, Simpson KW. 5-Aminosalicylic acid downregulates the growth and virulence of *Escherichia coli* associated with IBD and colorectal cancer, and upregulates host anti-inflammatory activity. *J Antibiot (Tokyo).* 2018;71(11):950–961. doi:10.1038/s41429-018-0081-8.
- Rubinstein MR, Wang X, Liu W, Hao Y, Cai G, Han YW. *Fusobacterium nucleatum* promotes colorectal carcinogenesis by modulating E-cadherin/beta-catenin signaling via its FadA adhesin. *Cell Host Microbe.* 2013;14(2):195–206. doi:10.1016/j.chom.2013.07.012.
- Suehiro Y, Sakai K, Nishioka M, Hashimoto S, Takami T, Higaki S, Shindo Y, Hazama S, Oka M, Nagano H, et al. Highly sensitive stool DNA testing of *Fusobacterium nucleatum* as a marker for detection of colorectal tumours in a Japanese population. *Ann Clin Biochem.* 2017;54(1):86–91. doi:10.1177/0004563216643970.
- Yu J, Chen Y, Fu X, Zhou X, Peng Y, Shi L, Chen T, Wu Y. Invasive *Fusobacterium nucleatum* may play a role in the carcinogenesis of proximal colon cancer through the serrated neoplasia pathway. *Int J Cancer.* 2016;139(6):1318–1326. doi:10.1002/ijc.30168.
- Yang Y, Weng W, Peng J, Hong L, Yang L, Toiyama Y, Gao R, Liu M, Yin M, Pan C, et al. *Fusobacterium nucleatum* increases proliferation of colorectal cancer cells and tumor development in mice by activating toll-like receptor 4 signaling to nuclear factor-kappaB, and up-regulating expression of MicroRNA-21. *Gastroenterology.* 2017;152(4):851–66 e24. doi:10.1053/j.gastro.2016.11.018.
- Wong SH, Kwong TNY, Chow TC, Luk AKC, Dai RZW, Nakatsu G, Lam TYT, Zhang L, Wu JCY, Chan FKL, et al. Quantitation of faecal *Fusobacterium* improves faecal immunochemical test in detecting advanced colorectal neoplasia. *Gut.* 2017;66(8):1441–1448. doi:10.1136/gutjnl-2016-312766.
- Castellarin M, Warren RL, Freeman JD, Dreolini L, Krzywinski M, Strauss J, Barnes R, Watson P, Allen-Vercos E, Moore RA, et al. *Fusobacterium nucleatum* infection is prevalent in human colorectal carcinoma. *Genome Res.* 2012;22(2):299–306. doi:10.1101/gr.126516.111.
- Ray K. Colorectal cancer: *Fusobacterium nucleatum* found in colon cancer tissue—could an infection cause colorectal cancer? *Nat Rev Gastroenterol Hepatol.* 2011;8(12):662. doi:10.1038/nrgastro.2011.208.
- Grivnenkov SI, Wang K, Mucida D, Stewart CA, Schnabl B, Jauch D, Taniguchi K, Yu GY, Osterreicher CH, Hung KE, et al. Adenoma-linked barrier defects and microbial products drive IL-23/IL-17-mediated tumour growth. *Nature.* 2012;491(7423):254–258. doi:10.1038/nature11465.
- Abed J, Emgard JE, Zamir G, Faroja M, Almogy G, Grenov A, Sol A, Naor R, Pikarsky E, Atlan KA, et al. Fap2 mediates *Fusobacterium nucleatum* colorectal adenocarcinoma enrichment by binding to

- tumor-expressed Gal-GalNAc. *Cell Host Microbe*. 2016;20(2):215–225. doi:[10.1016/j.chom.2016.07.006](https://doi.org/10.1016/j.chom.2016.07.006).
17. Kostic AD, Chun E, Robertson L, Glickman JN, Gallini CA, Michaud M, Clancy TE, Chung DC, Lochhead P, Hold GL, et al. *Fusobacterium nucleatum* potentiates intestinal tumorigenesis and modulates the tumor-immune microenvironment. *Cell Host Microbe*. 2013;14(2):207–215. doi:[10.1016/j.chom.2013.07.007](https://doi.org/10.1016/j.chom.2013.07.007).
 18. Mima K, Nishihara R, Qian ZR, Cao Y, Sukawa Y, Nowak JA, Yang J, Dou R, Masugi Y, Song M, et al. *Fusobacterium nucleatum* in colorectal carcinoma tissue and patient prognosis. *Gut*. 2016;65(12):1973–1980. doi:[10.1136/gutjnl-2015-310101](https://doi.org/10.1136/gutjnl-2015-310101).
 19. Yu T, Guo F, Yu Y, Sun T, Ma D, Han J, Qian Y, Kryczek I, Sun D, Nagarsheth N, et al. *Fusobacterium nucleatum* promotes chemoresistance to colorectal cancer by modulating autophagy. *Cell*. 2017;170(3):548–63 e16. doi:[10.1016/j.cell.2017.07.008](https://doi.org/10.1016/j.cell.2017.07.008).
 20. Li YY, Ge QX, Cao J, Zhou YJ, Du YL, Shen B, Wan YJ, Nie YQ. Association of *Fusobacterium nucleatum* infection with colorectal cancer in Chinese patients. *World J Gastroenterol*. 2016;22(11):3227–3233. doi:[10.3748/wjg.v22.i11.3227](https://doi.org/10.3748/wjg.v22.i11.3227).
 21. Yan X, Liu L, Li H, Qin H, Sun Z. Clinical significance of *Fusobacterium nucleatum*, epithelial-mesenchymal transition, and cancer stem cell markers in stage III/IV colorectal cancer patients. *Onco Targets Ther*. 2017;10:5031–5046. doi:[10.2147/OTT.S145949](https://doi.org/10.2147/OTT.S145949).
 22. Bullman S, Pedamallu CS, Sicinska E, Clancy TE, Zhang X, Cai D, Neuberg D, Huang K, Guevara F, Nelson T, et al. Analysis of *Fusobacterium* persistence and antibiotic response in colorectal cancer. *Science (New York, NY)*. 2017;358(6369):1443–1448. doi:[10.1126/science.aal5240](https://doi.org/10.1126/science.aal5240).
 23. Huang H, Cai L, Li R, Ye L, Chen Z. A novel lncRNA LOC101927746 accelerates progression of colorectal cancer via inhibiting miR-584-3p and activating SSRP1. *Biochem Biophys Res Commun*. 2019. doi:[10.1016/j.bbrc.2018.12.174](https://doi.org/10.1016/j.bbrc.2018.12.174).
 24. Yan Y, Wang Z, Qin B. A novel long noncoding RNA, LINC00483 promotes proliferation and metastasis via modulating of FMNL2 in CRC. *Biochem Biophys Res Commun*. 2018. doi:[10.1016/j.bbrc.2018.12.090](https://doi.org/10.1016/j.bbrc.2018.12.090).
 25. Huang B, Song JH, Cheng Y, Abraham JM, Ibrahim S, Sun Z, Ke X, Meltzer SJ. Long non-coding antisense RNA KRT7-AS is activated in gastric cancers and supports cancer cell progression by increasing KRT7 expression. *Oncogene*. 2016;35(37):4927–4936. doi:[10.1038/onc.2016.25](https://doi.org/10.1038/onc.2016.25).
 26. Grant CE, Bailey TL, Noble WS. FIMO: scanning for occurrences of a given motif. *Bioinformatics*. 2011;27(7):1017–1018. doi:[10.1093/bioinformatics/btr064](https://doi.org/10.1093/bioinformatics/btr064).
 27. Bailey TL, Boden M, Buske FA, Frith M, Grant CE, Clementi L, Ren J, Li WW, Noble WS, SUITE: MEME. tools for motif discovery and searching. *Nucleic Acids Res*. 2009;37:W202–8. WebServer issue. doi:[10.1093/nar/gkp335](https://doi.org/10.1093/nar/gkp335).
 28. Owens DW, Lane EB. The quest for the function of simple epithelial keratins. *Bioessays*. 2003;25(8):748–758. doi:[10.1002/bies.10316](https://doi.org/10.1002/bies.10316).
 29. Magin TM, Vijayaraj P, Leube RE. Structural and regulatory functions of keratins. *Exp Cell Res*. 2007;313(10):2021–2032. doi:[10.1016/j.yexcr.2007.03.005](https://doi.org/10.1016/j.yexcr.2007.03.005).
 30. Helfand BT, Chang L, Goldman RD. Intermediate filaments are dynamic and motile elements of cellular architecture. *J Cell Sci*. 2004;117(Pt 2):133–141. doi:[10.1242/jcs.00936](https://doi.org/10.1242/jcs.00936).
 31. Harbaum L, Pollheimer MJ, Kornprat P, Lindtner RA, Schlemmer A, Rehak P, Langner C. Keratin 7 expression in colorectal cancer – freak of nature or significant finding? *Histopathology*. 2011;59(2):225–234. doi:[10.1111/j.1365-2559.2011.03694.x](https://doi.org/10.1111/j.1365-2559.2011.03694.x).
 32. Bayrak R, Yenidunya S, Haltas H. Cytokeratin 7 and cytokeratin 20 expression in colorectal adenocarcinomas. *Pathol Res Pract*. 2011;207(3):156–160. doi:[10.1016/j.prp.2010.12.005](https://doi.org/10.1016/j.prp.2010.12.005).
 33. Li J, Lin S, Vanhoutte PM, Woo CW, Xu A. Akkermansia muciniphila protects against atherosclerosis by preventing metabolic endotoxemia-induced inflammation in apoe^{-/-} mice. *Circulation*. 2016;133(24):2434–2446. doi:[10.1161/CIRCULATIONAHA.115.019645](https://doi.org/10.1161/CIRCULATIONAHA.115.019645).
 34. Denman SE, McSweeney CS. Development of a real-time PCR assay for monitoring anaerobic fungal and cellulolytic bacterial populations within the rumen. *FEMS Microbiol Ecol*. 2006;58(3):572–582. doi:[10.1111/j.1574-6941.2006.00190.x](https://doi.org/10.1111/j.1574-6941.2006.00190.x).
 35. Yu YN, Yu TC, Zhao HJ, Sun TT, Chen HM, Chen HY, An HF, Weng YR, Yu J, Li M, et al. Berberine may rescue *Fusobacterium nucleatum*-induced colorectal tumorigenesis by modulating the tumor microenvironment. *Oncotarget*. 2015;6(31):32013–32026. doi:[10.18632/oncotarget.5166](https://doi.org/10.18632/oncotarget.5166).
 36. Kostic AD, Gevers D, Pedamallu CS, Michaud M, Duke F, Earl AM, Ojesina AI, Jung J, Bass AJ, Tabernero J, et al. Genomic analysis identifies association of *Fusobacterium* with colorectal carcinoma. *Genome Res*. 2012;22(2):292–298. doi:[10.1101/gr.126573.111](https://doi.org/10.1101/gr.126573.111).